Passivation of Metal Surface States: Microscopic Origin for Uniform Monolayer Graphene by Low Temperature Chemical Vapor Deposition

Insu Jeon,[†,§] Heejun Yang,[‡,§] Sung-Hoon Lee,[‡] Jinseong Heo,[‡] David H. Seo,[‡] Jaikwang Shin,[‡] U-In Chung,[‡] Zheong Gou Kim,[†] Hyun-Jong Chung,[‡,*] and Sunae Seo[‡,*]

[†]Department of Physics and Astronomy, Seoul National University, Seoul 151-747, Korea and [‡]Semiconductor Device Lab, Samsung Advanced Institute of Technology, Yongin 446-712, Korea.

[§] These authors contributed equally to this work

ABSTRACT Scanning tunneling microscopy (STM) and density functional theory (DFT) calculations were used to investigate the surface morphology and electronic structure of graphene synthesized on Cu by low temperature chemical vapor deposition (CVD). Periodic line patterns originating from the arrangements of carbon atoms on the Cu surface passivate the interaction between metal substrate and graphene, resulting in flawless inherent graphene band structure in pristine graphene/Cu. The effective elimination of metal surface states by the passivation is expected to contribute to the growth of monolayer graphene on Cu, which yields highly enhanced uniformity on the wafer scale, making progress toward the commercial application of graphene.

KEYWORDS: graphene · copper · scanning tunneling microscopy · density functional theory · chemical vapor deposition

Graphene, a single monolayer of graphite, has been attracting great interest in both basic science and industrial application.[1] Fundamental properties of this material have been explored mainly on exfoliated graphene with a maximum of hundreds of μm^2 area.[2] Besides exfoliated graphene flakes, graphene growth on SiC was performed for *in situ* analysis under ultrahigh vacuum (UHV) to reveal the high-resolution electronic structure of graphene.[3,4] Both of these methods offer only a limited area of graphene, and intensive effort has been devoted to developing a large-scale, high-throughput growth technique. The commercially feasible growth of graphene so that CMOS fabrication methods can be applied with large uniform area enough to integrate on silicon wafer was initiated by thermal CVD growth with hydrocarbon gas. This provides the chance to compete with silicon technology in manufacturing cost. Nevertheless, we need to further understand the role of substrates during the growth process[5,6] as well as how to control the uniformity and the number of graphene layers on the wafer scale.[7,8] In order to do that, the mechanism related to CVD growth at various conditions should be investigated through microscopic approach such as utilizing STM.

In CVD growth of graphene using a catalytic substrate, the quality of graphene largely relies on the substrate metal, temperature, and cooling rate.[8] The most successful growths were achieved on Ni and Cu substrates. The importance of the cooling rate associated with the segregation and precipitation process was addressed in Ni, one of the high carbon solubility metals, while surface reaction between substrate metal and hydrocarbon source was emphasized in Cu, which makes mostly single-layer graphene. It was also reported that the electronic density of states of graphene changes depending on the underlying metal due to the interaction with the substrate. The electronic structure of graphene grown on various metals has been studied by scanning tunneling microscopy (STM) or angle-resolved photoemission (ARPES).[9−14] From the previous studies, the measured electronic structure of graphene on Ni could be understood in terms of the strong interaction between graphene and substrate. However, graphene on noble metals such

* Address correspondence to sunaeseo@samsung.com, hyunjong.chung@samsung.com.

Received for review October 27, 2010 and accepted January 31, 2011.

Published online February 10, 2011
10.1021/nn102916c

as Pt or Cu, known to be weakly interacting between graphene and the substrate, was revealed to show features different from the intrinsic graphene band structure by scanning tunneling spectroscopy (STS).[15,16] This raises a fundamental question on how to interpret measured band structure coupled with substrate metallic states.

Here, we report an electronically decoupled graphene system on Cu(111) grown by low temperature CVD, showing the inherent Dirac cone near the Fermi level in STS. Density functional theory (DFT) calculations explain the measured STS data using a surface-modulated interface structure which provides the electronic detachment of graphene from Cu. Successive thermal treatment destroys this peculiar detachment by reconstructing the interface between graphene and Cu substrate and changes the electronic band structure of graphene into previously reported ones.

The growth substrate was prepared by depositing 500 nm thick Cu using electron-beam evaporation onto a SiO_2/Si wafer. After increasing the substrate temperature to 650 °C, hydrogen plasma was applied to clean the Cu surface. Then C_2H_2 and Ar gas were flowed with 100 W plasma power, and the graphene was grown during the dissociation of C_2H_2 for 3 min.[17,18] Unlike previous high temperature growth at ~1000 °C on Cu foil[7] or single crystal,[6,16] we adopted a plasma-supported growth to lower temperature. This unique synthesis by lowering temperature is a more practical approach because we avoid the melting point of Cu around 1000 °C in the fabrication process. The plasma helps to dissociate the C_2H_2 molecules. With this external active energy from the plasma, we could dissociate the hydrocarbon molecule at the low temperature of 650 °C, causing the graphene to weakly couple to the substrate. The grown graphene on Cu thin film was transferred to an STM chamber, and we took STM/STS measurements on the pristine graphene and repeated it after annealing the graphene at ~500 K for 24 h. Despite the polycrystalline character of the Cu film, the majority of Cu substrate was revealed to have (111) orientation by electron back-scattering diffraction (EBSD) measurement and STM images of neighbor steps of the Cu substrate.

RESULTS AND DISCUSSION

On the pristine graphene on Cu, we obtained a new incommensurate line structure, as shown by STM images in Figure 1a. This differs from the previously observed Moiré pattern.[16] The periodic lines separated by ~6.5 Å in pristine graphene are clearly seen over terraces, and 120°-rotated lines also exist on the same terrace. The direction of substrate steps indicates that the line patterns are generated on the Cu(111) domain as supported by EBSD data. The graphene continues to grow, covering the substrate steps. An atomic

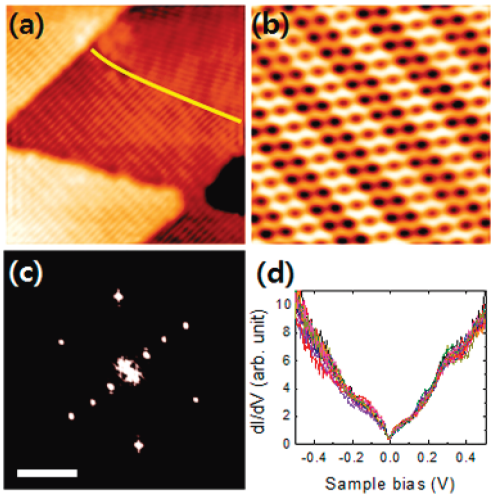

Figure 1. STM topography and d*I*/d*V* spectra of the graphene on line patterned Cu(111) synthesized by the CVD method at 650 °C. (a) 30 nm × 30 nm STM topography of the graphene. A domain boundary is highlighted with a yellow line. Tunneling condition: 0.5 V, 0.5 nA. (b) 3 n× 3 nm atomic resolution image of the lines covered by graphene. Tunneling condition: 1.0 V, 0.5 nA. (c) FT from the STM topography of panel b. Scale bar = 20 nm^{-1}. (d) d*I*/d*V* spectra across the lines or terraces.

resolution image of the line patterns and the corresponding Fourier transform (FT) in pristine graphene are shown in Figure 1b,c, respectively. Despite the low temperature during CVD, epitaxially grown graphene is clearly observed across the periodic line pattern, which is marked as two points near the Γ point. This superlattice structure covers most of the sample area, following the zigzag direction of the graphene and remains stable in the air at room temperature for several months.

In order to investigate the electronic structure of pristine graphene with the line patterns, STS was performed at the temperature of ~3 K by standard lock-in techniques to obtain dI/dV spectra over the region in Figure 1a. The STS in Figure 1d is completely different from the previously measured spectra of graphene on Cu(111) and other metals. Previous dI/dV spectra show the electronic structure of graphene, highly intermixed with metal surface states, or even dominated by the metallic surface structure.[15,16] However, our pristine graphene with line superstructure shows clear substrate-independent V-shape in STS, which is expected for ideal graphene. This is the first observation of the intrinsic electronic structure of graphene grown on metal. Interestingly, the dI/dV spectra are homogeneous across the line patterns and terraces of substrate, as shown in Figure 1d, implying that the electronic structure of the graphene is spatially uniform unlike epitaxial graphene on SiC.[19,20] STS results may include other effects such as phonon-assisted inelastic tunneling (see the Supporting Information), and the explanation of the STS will be discussed using a theoretical study later.

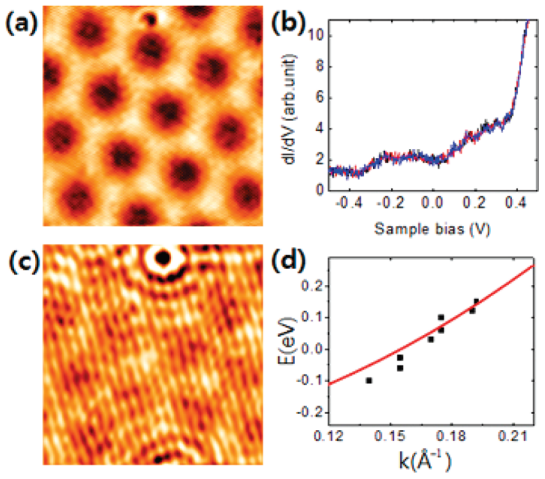

Figure 2. STM result on the graphene/Cu(111) annealed at 500 K. (a) 17 × 17 nm STM topography of the epitaxial graphene showing the Moiré pattern whose period is ~6.5 nm. Tunneling condition: 1.0 V, 0.5 nA. (b) d*I*/d*V*. (c) STM topography of the same region in panel a at low bias. Standing waves are observed near point defects indicating the probing of the surface states of Cu(111). Tunneling condition: 0.1 V, 0.5 nA. (d) Dispersion relation deduced from the variation of the wavelengths in panel c. The calculated effective mass is ~0.4 m_e.

After annealing the graphene sample at the temperature of ~500 K for ~24 h, the aforementioned line structures disappear and a Moiré pattern of large hexagons with the period of ~6.5 nm appears, as shown in Figure 2a, which is attributed to the discrepancy of lattice constants in hexagonal graphene and the Cu(111) surface. The appearance of a Moiré pattern by the thermal treatment accompanies the alteration of the dI/dV spectra, as shown in Figure 2b. At low bias regimes below 0.3 V, as in Figure 2c, the graphene is electronically transparent and the metallic surface of Cu(111) is visible in STM. The electronic standing waves near point defects are a key feature of the unperturbed surface states of Cu(111). With the varying wavelength of the standing wave, we deduced the dispersion relation of the surface state electrons under the graphene in Figure 2d. Despite the limited energy window due to the appearance of graphene's density of states at higher energies, we could obtain the dispersion curve with a similar effective electron mass (~0.40 m_e) as in clean Cu(111).[21] From the above analysis, we explain the altered STS as an observation of the Cu(111) surface state through the graphene.

To understand the STM/STS of graphene before and after annealing, we performed DFT calculations employing the local density approximation[22] and the projector-augmented wave method as implemented in VASP.[23,24] Valence electronic wave functions are expanded in a plane wave basis set with a cutoff energy of 273 eV. The Cu(111) surface is modeled by periodic Cu slabs, each of four atomic layers thick, separated by a vacuum spacing of ~10 Å. To simulate graphene on the Cu(111) surface, where the mismatch in the experimental lattice constants is as high as about 4%, we use the graphene $(3/\sqrt{3} \times 3/\sqrt{3})R30°$ supercell on the Cu(111)-(5 × 5) supercell so that the resulting lattice mismatch is below 1%. This combination is also taken to explain the period of the line patterns in our pristine graphene before annealing. The Brillouin zone integration is made with a uniform (6 × 6 × 1) mesh. All atoms except for the bottom Cu layer are relaxed until all of the residual forces are less than 0.02 eV/ Å.

The proposed model for the pristine graphene is described in Figure 3a, where the line patterns are introduced by modulating the top layer of the Cu substrate. As the origin of the surface modulation, an insertion of other elements into the top-layer Cu was adopted, which can effectively reduce the density of states of the surface states according to DFT calculation. The structure was based on Cu(111)-(5 × 5) supercell, and feasible elements such as H or C were selected as the insertion elements. The structure with the additional C atoms reproduces well the period (~6.4 Å) and the direction of line patterns shown in STM images. The distance between the graphene and the substrate Cu atoms is ~3.0 Å, big enough to maintain the linear dispersion of graphene. The structures without the C atoms or with H atoms instead, on the other hand, show a strong graphene−substrate interaction with a reduced spacing between them of 2.2−2.4 Å, failing to account for the linear experimental dI/dV spectra (Supporting Information). Other possibilities such as the Cu(100) or (110) surface as the substrate, the edge-, or strain-induced reconstruction of the Cu(111) surface, the linear Moiré pattern from a cubic Cu lattice,[25] and the regular surface dislocation or reconstruction have been considered, but found not to reproduce both the period and uniformity of the line patterns and the weak graphene−substrate interaction (Supporting Information). For the annealed graphene/Cu surface, a substrate reconstruction to the full-coverage Cu surface was assumed, as shown in Figure 3d, where the equilibrium graphene−substrate distance is calculated to be ~3.2 Å.

The difference of STS in pristine and annealed graphene/Cu system comes from two major physical quantities: intensity of projected density of states (PDOS) and spatial extension of involved wave functions. In the pristine graphene/Cu (Figure 3b), the PDOS of π bands of graphene (C 2p$_z$) is larger than the PDOS of Cu surface states (Cu 4p$_z$), and the modification of the electronic structure of graphene is negligible. However, the PDOS of the Cu(111) surface state exceeds the PDOS of the graphene π band around the Dirac point in the annealed graphene, as shown in Figure 3d. The amplitudes of the atomic wave functions in the vertical direction are shown in Figure 3e, where the distance of 3 Å between graphene and Cu is reflected. It is noticeable that the underlying Cu surface state largely extends in the upward

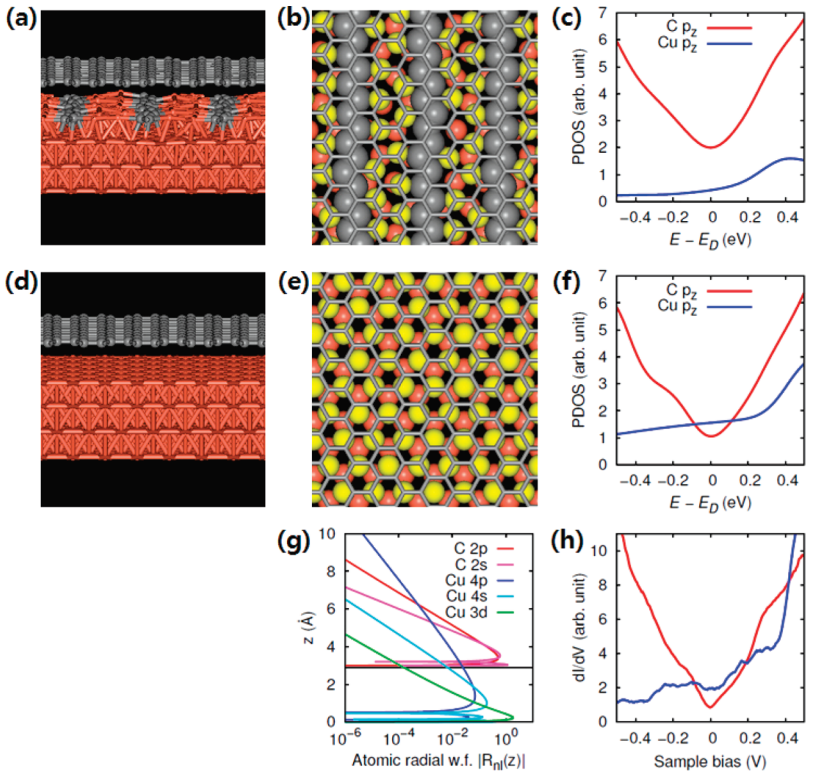

Figure 3. Calculated atomic and electronic structures for the pristine and annealed graphene/Cu(111) surfaces. (a,d) Prospective views of the structural models of the pristine and annealed surfaces. Gray and red spheres are C and Cu atoms, respectively. (b,e) Top views of the structural models. The graphene layer is depicted as a honeycomb network of gray sticks, and the yellow and red spheres are the first- and second-layer Cu atoms, respectively. The gray spheres in (b) are the inserted C atoms. (c,f) PDOS of the graphene C $2p_z$ states and the top-layer Cu $4p_z$ states of the structural models. (g) Spatial extent of atomic radial wave functions. The wave functions of the C atom are 3 Å upward shifted to reflect the graphene−substrate separation. (h) Experimental d*I*/d*V* data of the pristine (red line) and annealed (blue line) graphene/Cu(111) surfaces.

direction (blue curve). In the pristine graphene/Cu system, the intrinsic band structure of graphene is obtained due to the relatively large PDOS of graphene π bands (Figure 3b), while the extended tails of Cu surface states are probed by STM due to the relatively small PDOS of graphene π band (Figure 3d) in the annealed graphene/Cu system.

The two distinct systems of graphene on Cu are described schematically in Figure 4. Gray spheres are carbon atoms, and the vertical extension of the atomic wave function (C $2p_z$) is represented as gray ellipses. Orange spheres represent Cu atoms, and they show long atomic wave function (Cu $4p_z$) in both systems. Dark and bright orange ellipses indicate the relatively large and small PDOS of Cu surface state near the Fermi energy, respectively. In Figure 4a, it is clearly seen that the STM tip probes mainly the graphene electronic structure as the gray ellipses are dominant compared to the bright orange ellipses, reducing the catalytic function of Cu. On the other hand, dark orange ellipses are extended over graphene wave function in Figure 4b, which implies that the STM tip probes mainly the Cu surface state.

Finally, we want to underline that the quality of our CVD graphene on Cu at low temperature is distinguished, compared to graphene grown at high temperature.

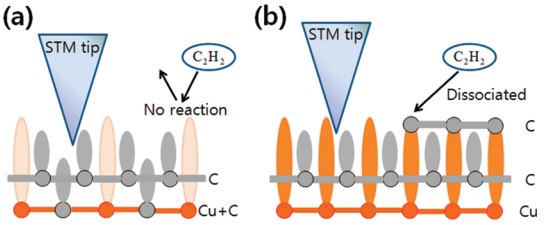

Figure 4. Schematic pictures for the two systems of graphene/Cu. Gray spheres are carbon atoms and orange spheres are Cu atoms. (a) Bright orange ellipse indicates the small PDOS of Cu surface state. STM tip probes both gray and orange ellipse, but the C atomic wave function dominates the measurement. During the growth process, C_2H_2 molecules are not dissociated to make the second layer of graphene because of the weak catalytic effect of Cu substrate. (b) In high temperature CVD processes done by other groups, Cu atomic wave function penetrates the graphene layer, so that additional partial layers of graphene may be grown. The Cu atomic wave function dominates STM measurement, as shown by dark orange ellipses close to the STM tip. This explains the STS results showing the Cu surface state in previous studies and in our annealed graphene.

It has been reported that higher order layer shows slower growth rate due to a much lower concentration of Cu catalyst available to promote the decomposition of hydrocarbon gas so that the graphene multilayers cover a small area regime of 5%, which is a tremendous advantage of single-layer graphene grown on Cu.[26] In

our epitaxial graphene grown at low temperature, no sign of the evolution into even a bilayer or triple layer was recognized.[15] Any contrast change comparable to the multilayer was not detected in the optical image or Raman spectral spatial mapping in the intensity ratio of 2D/G or half-width at half-maximum (hwhm) of 2D as well as having an optical transmittance of 97.7% at 550 nm. Here G and 2D, conventional notations, are the zone center phonon and the overtone of K point phonon, respectively. The blockage of Cu electronic states by the graphene layer should help the growth of uniform single graphene, as shown in Figure 4. In addition, naturally occurring byproduct, like ripples owing to the high temperature process, does not exist in our single-layer graphene. We believe that this low temperature process could give us the chance to improve device quality with enhanced electronic properties of graphene and develop mass producible commercial products using a top-down CMOS compatible approach.

CONCLUSION

In summary, we investigated the graphene/Cu(111) system grown at low temperature by a plasma-assisted CVD method using STM/STS and theoretical DFT calculations. A line patterned superstructure and inherent graphene electronic structure were measured in the pristine graphene/Cu, whereas Moiré pattern and Cu surface states were observed in annealed graphene. DFT calculations were performed on the two systems, and the modulation of the Cu surface layer underneath graphene was suggested to explain the result. The first observation of electronically detached single-layer graphene in STS, without introducing artificial intercalation, is a singular consequence of the low temperature CVD process on the graphene/metal system. The reduced influence of Cu surface prevents further growth of graphene, which can be used for fabricating a large homogeneous single layer of graphene.

METHODS

Sample fabrication was done by preparing 500 nm thick Cu using electron-beam evaporation onto a SiO_2/Si wafer. We used this substrate for growth of graphene layers using plasma-enhanced chemical vapor deposition (PECVD). In the PECVD chamber, we first increased the substrate temperature to 650 °C, then hydrogen gas was flowed into the chamber while and external RF coil was used to induce the plasma to clean the Cu surface. The pressure during this step was kept at 50 mTorr, while the hydrogen gas flow rate was 40 sccm, and the RF forward power was 100 W. Then, C_2H_2 at 1 sccm and Ar gas at 40 sccm were flowed with 100 W plasma power. The graphene was grown during the dissociation of C_2H_2 for 3 min. The low temperature of 650 °C caused the graphene to weakly couple to the substrate. The grown graphene on Cu thin film was transferred to an STM chamber, and we took STM/STS measurements on the pristine graphene and repeated it after annealing the graphene at ~500 K for 24 h.

Acknowledgment. We thank Y. Kuk in Seoul National University for helpful discussions.

Supporting Information Available: Four figures and expanded discussions of peripheral findings. This material is available free of charge via the Internet at http://pubs.acs.org

REFERENCES AND NOTES

1. Geim, A. K.; Novoselov, K. S. The Rise of Graphene. *Nat. Mater.* **2007,** *6*, 183–191.
2. Zhang, Y.; Tan, Y.-W.; Stormer, H. L.; Kim, P. Experimental Observation of the Quantum Hall Effect and Berry's Phase in Graphene. *Nature* **2005,** *438*, 201–204.
3. Berger, C.; Song, Z.; Li, X.; Wu, X.; Brown, N.; Naud, C.; Mayou, D.; Li, T.; Hass, J.; Marchenkov, A. N.; *et al.* Electronic Confinement and Coherence in Patterned Epitaxial Graphene. *Science* **2006,** *312*, 1191–1196.
4. Yang, H.; Mayne, A. J.; Boucherit, M.; Comtet, G.; Dujardin, G.; Kuk, Y. Quantum Interference Channeling at Graphene Edges. *Nano Lett.* **2010,** *10*, 943–947.
5. Gao, M.; Pan, Y.; Zhang, C.; Hu, H.; Yang, R.; Lu, H.; Cai, J.; Du, S.; Liu, F.; Gao, H. J. Tunable Interfacial Properties of Epitaxial Graphene on Metal Substrates. *Appl. Phys. Lett.* **2010,** *96*, 053109.
6. Cao, H.; Yu, Q.; Jauregui, L. A.; Tian, J.; Wu, W.; Liu, Z.; Jalilian, R.; Benjamin, D. K.; Jiang, Z.; Bao, J.; *et al.* Electronic Transport in Chemical Vapor Deposited Graphene Synthesized on Cu: Quantum Hall Effect and Weak Localization. *Appl. Phys. Lett.* **2010,** *96*, 122106.
7. Li, X.; Cai, W.; An, J.; Kim, S.; Nah, J.; Yang, D.; Piner, R.; Velamakanni, A.; Jung, I.; Tutuc, E.; *et al.* Large-Area Synthesis of High-Quality and Uniform Graphene Films on Copper Foils. *Science* **2009,** *324*, 1312–1314.
8. Lee, S.; Lee, K.; Zhong, Z. Wafer Scale Homogeneous Bilayer Graphene Films by Chemical Vapor Deposition. *Nano Lett.* **2010,** *10*, 4702–4707.
9. Wintterlin, J.; Bocquet, M.-L. Graphene on Metal Surfaces. *Surf. Sci.* **2009,** *603*, 1841–1852.
10. Preobrajenski, A. B.; Ng, M. L.; Vinogradov, A. S.; Mårtensson, N. Controlling Graphene Corrugation on Lattice-Mismatched Substrates. *Phys. Rev. B* **2008,** *78*, 073401.
11. Sutter, P.; Sadowski, J. T.; Sutter, E. Graphene on Pt(111): Growth and Substrate Interaction. *Phys. Rev. B* **2009,** *80*, 245411.
12. Sutter, P.; Flege, J.; Sutter, E. Epitaxial Graphene on Ruthenium. *Nat. Mater.* **2008,** *7*, 406–411.
13. Coraux, J.; N'Diaye, A. T.; Busse, C.; Michely, T. Structural Coherency of Graphene on Ir(111). *Nano Lett.* **2008,** *8*, 565–570.
14. Gruneis, A.; Kummer, K.; Vyalikh, D. Dynamics of Graphene Growth on a Metal Surface: A Time-Dependent Photoemission Study. *New J. Phys.* **2009,** *11*, 073050.
15. Levy, N.; Burke, S. A.; Meaker, K. L.; Panlasigui, M.; Zettl, A.; Guinea, F.; Neto, A.; Crommie, M. F. Strain-Induced Pseudo-magnetic Fields Greater Than 300 T in Graphene Nanobubbles. *Science* **2010,** *329*, 544–547.
16. Gao, L.; Guest, J. R.; Guisinger, N. P. Epitaxial Graphene on Cu(111). *Nano Lett.* **2010,** *10*, 3512–3516.
17. Lee, J.; Chung, H.-J.; Lee, J.; Shin, H.; Heo, J.; Yang, H.; Lee, S.-H.; Seo, S.; Shin, J.; Chung, U.-I.; Yoo, I.; Kim, K. RF Performance of Pre-patterned Locally-Embedded-Back-Gate Graphene Device. *Int. Electron Devices Meet.* **2010,** *23*, 5.
18. Heo, J.; Chung, H.-J.; Lee, S.-H.; Yang, H.; Seo, D. H.; Shin, J. K.; Chung, U.; Seo, S.; Hwang, E. H.; Das Sarma, S. Nonmonotonic Temperature Dependent Transport in Graphene Grown by Chemical Vapor Deposition. arXiv:1009.2506v1 [cond-mat.mes-hall].
19. Brar, V. W.; Zhang, Y.; Yayon, Y.; Ohta, T.; McChesney, J. L.; Bostwick, A.; Rotenberg, E.; Horn, K.; Crommie, M. F.

Scanning Tunneling Spectroscopy of Inhomogeneous Electronic Structure in Monolayer and Bilayer Graphene on SiC. *Appl. Phys. Lett.* **2007,** *91*, 122102.
20. Yang, H.; Baffou, G.; Mayne, A. J.; Comtet, G.; Dujardin, G.; Kuk, Y. Topology and Electron Scattering Properties of the Electronic Interfaces in Epitaxial Graphene Probed by Resonant Tunneling Spectroscopy. *Phys. Rev. B* **2008,** *78*, 041408(R).
21. Park, J.; Ham, U.; Kahng, S.; Kuk, Y.; Miyake, K.; Hata, K.; Shigekawa, H. Modification of Surface-State Dispersion upon Xe Adsorption: A Scanning Tunneling Microscope Study. *Phys. Rev. B* **2000,** *62*, R16341–R16344.
22. Perdew, J. P.; Zunger, A. Self-Interaction Correction to Density-Functional Approximations for Many-Electron Systems. *Phys. Rev. B* **1981,** *23*, 5048–5079.
23. Kresse, G.; Furthmüller, J. Efficient Iterative Schemes for *Ab Initio* Total-Energy Calculations Using a Plane-Wave Basis Set. *Phys. Rev. B* **1996,** *54*, 11169–11186.
24. Kresse, G.; Joubert, D. From Ultrasoft Pseudopotentials to the Projector Augmented-Wave Method. *Phys. Rev. B* **1999,** *59*, 1758–1775.
25. Zhao, L.; Rim, K. T; Zhou, H.; He, R.; Heinz, T. F.; Pinczuk, A.; Flynn, G. W.; Pasupathy, A. N. The Atomic-Scale Growth of Large-Area Monolayer Graphene on Single-Crystal Copper Substrates. arXiv:1008.3542v1
26. Li, X.; Cai, W.; Colombo, L.; Ruoff, R. S. Evolution of Graphene Growth on Ni and Cu by Carbon Isotope Labeling. *Nano Lett.* **2009,** *9*, 4268–4272.